nature geoscience

LETTERS

PUBLISHED ONLINE: 2 MARCH 2015 | DOI: 10.1038/NGEO2369

Impact vaporization of planetesimal cores in the late stages of planet formation

Richard G. Kraus[1,2*], Seth Root[3], Raymond W. Lemke[4], Sarah T. Stewart[1,5], Stein B. Jacobsen[1] and Thomas R. Mattsson[4]

Differentiated planetesimals delivered iron-rich material to the Earth and Moon in high-velocity collisions at the end stages of accretion. The physical process of accreting this late material has implications for the geochemical evolution of the Earth–Moon system and the timing of Earth's core formation[1–3]. However, the fraction of a planetesimal's iron core that is vaporized by an impact is not well constrained as a result of iron's poorly understood equation of state. Here we determine the entropy in the shock state of iron using a recently developed shock-and-release experimental technique implemented at the Sandia National Laboratory Z-Machine. We find that the shock pressure required to vaporize iron is 507 (+65, −85) GPa, which is lower than the previous theoretical estimate[4] (887 GPa) and readily achieved by the high velocity impacts at the end stages of accretion. We suggest that impact vaporization of planetesimal cores dispersed iron over the surface of the growing Earth and enhanced chemical equilibration with the mantle. In addition, the comparatively low abundance of highly siderophile elements in the lunar mantle and crust[5–8] can be explained by the retention of a smaller fraction of vaporized planetesimal iron on the Moon, as compared with Earth, due to the Moon's lower escape velocity.

Estimates of the timing of the end of Earth's core formation range from ∼30 to >100 Myr after the start of the Solar System[2] and depend on approximations for the magnitude of metal–silicate chemical equilibration for impactors of different sizes and impact velocities. Complete equilibration via emulsification of iron in a mantle magma ocean may occur by mixing the core material to centimetre length scales[9]. However, numerical simulations of giant impacts generally find that the impactor's core penetrates through the mantle to Earth's core[10,11], and calculations of Rayleigh–Taylor instabilities and turbulent mixing do not achieve emulsification of iron cores larger than about 10 km (ref. 12). Even when cores are emulsified by instabilities, they may only equilibrate with a fraction of Earth's mantle unless there is significant post-emulsification mixing[12]. Thus, studies of the physics of core formation have suggested limited chemical equilibration of impactor cores with Earth's mantle. In contrast, chemical[1] and W-isotopic evidence[2] suggest that more substantial equilibration must have occurred.

Core formation removes highly siderophile elements (HSEs: Re, Os, Ir, Ru, Rh, Pt, Pd, Au) from the mantle, but Earth's mantle contains orders of magnitude higher concentrations of HSEs than predicted by their low-pressure metal–silicate partitioning coefficients[6,13]. The concentrations and chondritic proportions of HSEs in the mantles of the Earth, Moon and other planets are used to infer the late accretion of chondritic planetesimals throughout the inner Solar System[3,13]. Perplexingly, the abundance of HSEs in the lunar mantle and crust has been estimated to be about one to two orders of magnitude smaller than expected[5,6,8] if the Moon accreted the same population of late impactors as Earth, adjusted for their gravitational capture cross-sections. To explain the low abundance of HSEs on the Moon, recent studies have proposed dynamical solutions, including enhanced gravitational focusing of slow, small (∼10 m) planetesimals onto the Earth[8] or the stochastic accretion of a few large (∼1,000 km) planetesimals to the Earth but not the Moon[14]. However, *N*-body simulations of the end stages of terrestrial planet formation find that the impact velocities of late-accreting planetesimals are very large (one to four times Earth's escape velocity)[15,16], and collisions between planetesimals are erosive[17], leading to a size distribution of small bodies rather than a few large planetesimals. So far, the role of impact-induced vaporization of iron cores during core formation and late accretion has not been investigated.

The shock pressure required for the onset of vaporization on decompression is determined by comparing the entropy on the Hugoniot to the entropy of vaporization at ambient pressures[18]. In general, the entropy on the Hugoniot has been estimated by theoretical equation of state (EOS) models. However, the entropy on the Hugoniot may be determined more accurately by combining shock temperature measurements with thermodynamic data from lower pressures and temperatures[19]. Although shock temperature measurements are relatively straightforward on transparent materials, shock temperature measurements on opaque materials are much more difficult to carry out accurately (see ref. 20 for an excellent review). Consequently, experimentally constrained thermodynamic integrations cannot be performed to determine the entropy along the Hugoniot of opaque solids such as iron, and the thermal EOS of opaque solids are generally poorly known.

Here, we developed an experimental technique to determine the entropy on the iron Hugoniot and derive the shock pressure required for vaporization of iron. The entropy at a point on the iron Hugoniot was determined by finding the shock pressure where the release isentrope intersects the 1-bar boiling point on the liquid–vapour phase boundary, where the entropy is experimentally constrained. The critical release isentrope was identified by measuring the density of iron at the state where the isentrope intersects the liquid branch of the liquid–vapour phase boundary (Supplementary Information and ref. 19).

[1]Department of Earth and Planetary Sciences, Harvard University, 20 Oxford Street, Cambridge, Massachusetts 02138, USA. [2]Shock Physics Group, Lawrence Livermore National Laboratory, PO Box 808, L-487, Livermore, California 94551-0808, USA. [3]Dynamic Material Properties Group, Sandia National Laboratory, PO Box 5800, Albuquerque, New Mexico 87185-1195, USA. [4]High Energy Density Physics Theory, Sandia National Laboratory, PO Box 5800, Albuquerque, New Mexico 87185-1189, USA. [5]Department of Earth and Planetary Sciences, UC Davis, One Shields Avenue, Davis, California 95616, USA. *e-mail: kraus4@llnl.gov

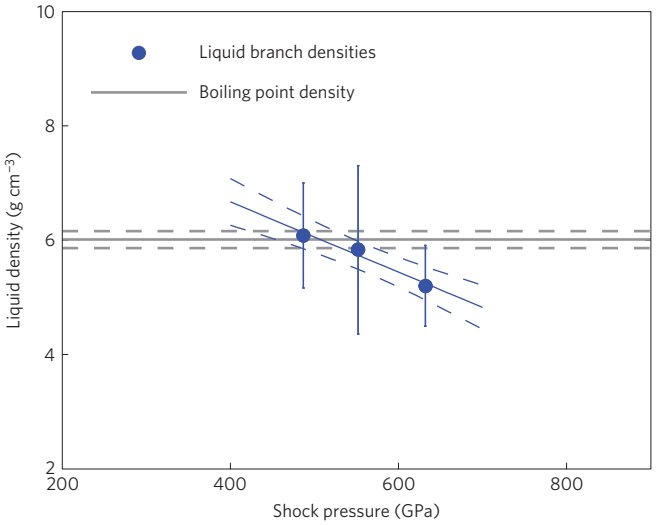

Figure 1 | Liquid densities as a function of shock pressure. Measured density of iron isentropically decompressed to the liquid–vapour phase boundary from a shock state on the principal Hugoniot (points with error bars) and the density of liquid iron at the 1-bar boiling point (grey line and dashed lines; refs 21,22 and Supplementary Information). The intersection between the release density trend (solid blue line and blue dashed lines) and the density at the boiling point determines the critical shock pressure to release to incipient vaporization.

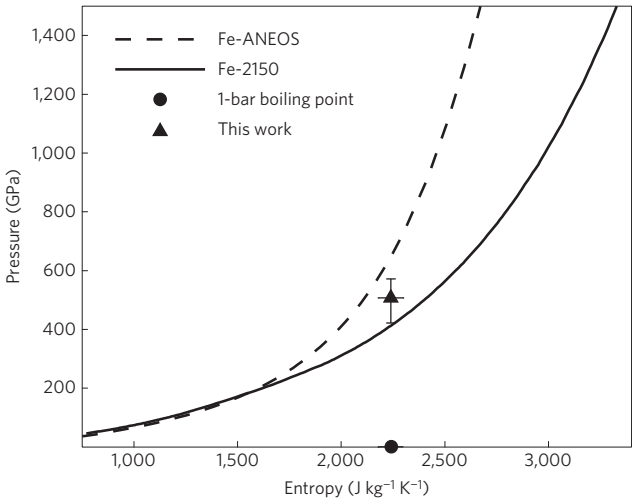

Figure 2 | Entropy on the iron Hugoniot. Comparison of the SESAME 2150 EOS for iron[23], the ANEOS EOS for iron[25], and our data point (with error bars) for the entropy on the iron Hugoniot. Also shown is the entropy at the 1-bar boiling point (Supplementary Information).

In Fig. 1, the measured density on the liquid branch of the liquid–vapour phase boundary of iron is presented as a function of the shock pressure achieved in the iron sample. The intersection of the data and the 1-bar boiling point density of liquid iron[21,22] represents the shock pressure required for the release path to intersect the boiling point. Thus, we have experimentally linked the thermodynamic state at the 1-bar boiling point to the principal Hugoniot via the release isentrope. There are sufficient heat capacity measurements on iron at 1 bar to perform an experimentally constrained thermodynamic integration from 0 K to the boiling point temperature, 3,133 ± 70 K, to calculate the entropy at the boiling point, 2,240 ± 60 J kg^{-1} K^{-1} (Supplementary Information). We find that the 1-bar boiling point entropy is achieved at 507(+65, −85) GPa on the iron principal Hugoniot. Hence, the shock pressure in iron required for the onset of vaporization on decompression to 1 bar is 507(+65, −85) GPa.

Our experimentally determined shock pressure required for incipient vaporization of iron is significantly lower than a widely used theoretical estimate of 887 GPa (ref. 4). There are large differences between our result and the entropies on the most common theoretical Hugoniots used for planetary science and physics applications, shown in Fig. 2. The entropy along the iron Hugoniot by ref. 23 is too high, which is consistent with the model's melting temperatures being lower than recent experiments[24]. The entropy on the ANEOS Hugoniot for iron[25] is too low and predicts a shock pressure required for incipient vaporization that is too high, ~635 GPa. These EOS models were developed without experimental constraints on the temperature or the entropy along the Hugoniot. Our data will significantly improve future EOS models at the high pressures critical for modelling planetary impacts and interiors.

The entropy on the Hugoniot is a critical parameter for understanding shock-induced phase changes during planetary impact events. Using our data and a series of high-resolution three-dimensional impact simulations (Supplementary Information), we are able to determine the required impact velocity for a differentiated impactor that will lead to vaporization of the iron core on decompression to 1 bar. The impact velocity depends on impact angle, but we find that the iron cores transition from no vaporization to partial vaporization of most of the impacting cores between ~15–20 km s^{-1} for an initial temperature of 1,500 K. Then using the lever rule and the 1-bar entropies for incipient and complete vaporization, the approximate percentage of vaporized iron core is determined as a function of the impact velocity of a differentiated impactor colliding with the proto-Earth mantle, shown in Fig. 3a.

To place the required impact velocity for vaporization into context, we compare our results to the distribution of planetesimal impact velocities onto Earth-mass planets from *N*-body simulations of terrestrial planet formation[16], which are representative of impact velocities during the end stages of accretion (Fig. 3b). Vaporization of iron (>~18 km s^{-1}) was achieved by 70% of planetesimal collisions onto the Earth and ~55% of collisions onto the Moon, where the lunar impact velocity distribution is estimated from the terrestrial distribution. Vaporization of undifferentiated planetesimals can be estimated by the onset of vaporization of silica (~8 km s^{-1}; Supplementary Information and ref. 19), which was achieved by ~90% of planetesimal impacts onto the Moon. The onset of vaporization is accompanied by a large volume change associated with adiabatic expansion that accelerates core material away from the impact site[26]. The expansion velocities for partially vaporized iron and silicate exceed the escape velocity of the Moon (2.4 km s^{-1}) but not Earth. Thus, the onset of vaporization leads to an abrupt and substantial decrease in the fraction of projectile accreted to the Moon. Including the effects of vaporization of high-velocity planetesimals, the decrease in shock pressures at oblique impact angles, and gravitational focusing of low-velocity planetesimals, the ratio of mass accreted to the Earth and Moon ranges from about 50 to 900 (Supplementary Information). Based on the observations of the HSEs, the late accreted mass ratio is estimated to fall between 100 and 2,700 (refs 6,8,13). Thus, shock-induced vaporization and escape by adiabatic expansion can account for the lower range of estimated abundances of HSEs on the Moon, and novel dynamical conditions[8,14] are not required.

Before the late accretion of HSEs, impact vaporization changed the way iron was incorporated into the growing Earth. Shock compression and subsequent decompression to a state of vaporization will generate a size distribution of small particles[26]

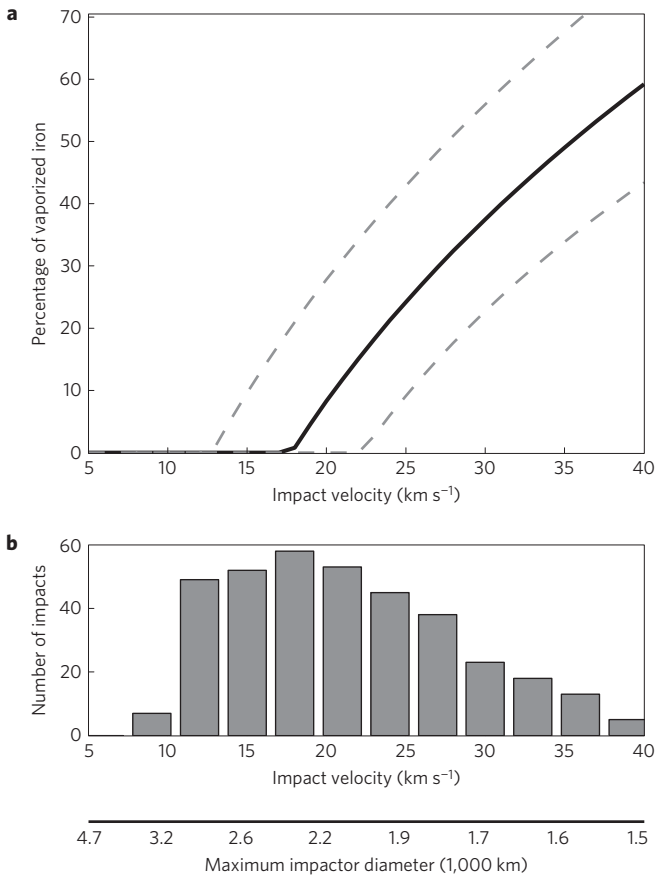

Figure 3 | Iron vaporization fraction during planet formation. **a**, Angle-averaged peak vaporization fraction of iron cores as a function of impact velocity for a 1,500 K initial temperature (solid line) with the 1σ confidence interval (dashed lines) resulting from the uncertainty in the entropy and the variance in the impact angle dependence. **b**, Histogram of impact velocities onto Earth-mass planets from *N*-body simulations of planet formation[16]. At each impact velocity, bodies larger than the estimated maximum impactor diameter may penetrate through Earth's mantle to the core (Supplementary Information). The onset of vaporization aids the dispersal of the cores of impactors smaller than this size limit.

(~mm to cm scale). These particles are distributed globally via adiabatic expansion of the decompressing projectile material and are small enough to equilibrate with a magma ocean[9]. The enhanced dispersal increases the volume of Earth's mantle that interacts with each impactor core. Thus, for impactors with diameters up to ~2,600 km (Fig. 3b) and impact velocities above ~18 km s^{-1} (and at lower velocities if silicate vapour entrains iron fragments), impact vaporization will significantly enhance core comminution and dispersal over the surface of the growing planet (Supplementary Information). Previous physical models of iron core breakup, without impact vaporization, found that only iron bodies smaller than about 10 km in size fully equilibrate[12]. With vaporization, the range of parameter space for metal–silicate equilibration is much larger and encompasses most planetesimal impacts during planet formation[15,16]. The onset of vaporization provides a physical mechanism in support of geochemical arguments that moderately siderophile element abundances in Earth's mantle are not inherited from planetesimal mantles[1] and substantial re-equilibration occurred on the growing Earth.

The effect of impact vaporization on the timing of accretion and core formation can be substantial. During the giant impact stage of planet formation[15,16], planetesimals deliver about half of the accreted mass, and about 30% and 80% of all planetesimal impacts onto the growing terrestrial planets reach the onset of vaporization for iron cores and silicates, respectively. As the fraction of equilibrated impactor material increases, the timescale for accretion shifts from the endmember local equilibrium model[27], with a mean time of core formation of 115 Myr, towards the magma ocean model[28], with a mean time of 11 Myr. Hence, a 10% increase in the fraction of accreted mass that globally equilibrates via vaporization will decrease the calculated time of accretion/core formation by ~10 Myr (Supplementary Information). Although the magnitude of metal–silicate equilibration during giant impacts is uncertain[12], most of the accreted planetesimals are expected to equilibrate with the growing planet.

The shock-and-release experiments described here traverse a wide range of states within the warm dense matter (WDM) region of phase space. WDM is exceptionally difficult to explore experimentally and complicated to model from first principles; yet, reliable descriptions of the WDM region are needed for accurate simulations of the most pressing problems in shock physics and planetary science. Our experimental techniques to measure the density on the liquid–vapour phase boundary and the entropy on the Hugoniot provide an extremely sensitive test for the theoretical models employed in EOS development. These techniques are completely general, and we anticipate they will be used to probe the poorly understood regions of the EOS for a wide range of elements and compounds of key importance in physics, geophysics and planetary science.

Methods

Sandia National Laboratory's Z machine[29] was used to launch aluminium flyer plates onto ~200-μm-thick samples of iron, generating a steady, planar shock wave with amplitudes between 487 and 632 GPa, significantly greater than what is achievable on a two-stage gas gun[30] yet with similar accuracy. On the shock wave reaching the downrange free surface of the iron sample, a rarefaction wave propagates back into the sample, simultaneously accelerating and decompressing the iron along an isentropic path from the Hugoniot state to zero pressure. Owing to the discontinuous change in sound velocity at the intersection of the isentrope with the liquid–vapour phase boundary, the rarefaction wave splits into two separate waves, generating a region of material between the two waves that is inertially trapped on the liquid branch of the liquid–vapour phase boundary. The decompressing iron expands uniaxially across a gap of known distance and impacts a standard window. The density of the inertially trapped liquid is determined by measuring the steady shock state generated in the window, as in a reverse impact experiment (see Supplementary Information and ref. 19 for experimental details and development of the technique).

Received 22 September 2014; accepted 19 January 2015; published online 2 March 2015

References

1. Rubie, D. C., Nimmo, F. & Melosh, H. J. *Treatise on Geophysics* Vol. 9, 51–90 (Elsevier, 2007).
2. Kleine, T. *et al.* Hf-W chronology of the accretion and early evolution of asteroids and terrestrial planets. *Geochim. Cosmochim. Acta* **73,** 5150–5188 (2009).
3. Day, J. M. D., Walker, R. J., Qin, L. & Rumble, D. Late accretion as a natural consequence of planetary growth. *Nature Geosci.* **5,** 614–618 (2012).
4. Pierazzo, E., Vickery, A. & Melosh, H. J. A reevaluation of impact melt production. *Icarus* **127,** 408–423 (1997).
5. Walker, R. J., Horan, M. F., Shearer, C. K. & Papike, J. J. Depletion of highly siderophile elements in the lunar mantle: Evidence for prolonged late accretion. *Earth Planet. Sci. Lett.* **224,** 399–413 (2004).
6. Day, J. M. D., Pearson, D. G. & Taylor, L. A. Highly siderophile element constraints on accretion and differentiation on the Earth–Moon system. *Science* **315,** 217–219 (2007).
7. Day, J. M. D., Walker, R. J., Odette, J. B. & Puchtel, I. S. Osmium isotope and highly siderophile element systematics of the lunar crust. *Earth Planet. Sci. Lett.* **289,** 595–605 (2010).
8. Schlichting, H. E., Warren, P. H. & Yin, Q. Z. The last stages of terrestrial planet formation: Dynamical friction and the late veneer. *Astrophys. J.* **752,** 8 (2012).

9. Rubie, D. C., Melosh, H. J., Reid, J. E., Liebske, C. & Righter, K. Mechanisms of metal–silicate equilibration in the terrestrial magma ocean. *Earth Planet. Sci. Lett.* **205,** 239–255 (2003).
10. Canup, R. M. Forming a Moon with an Earth-like composition via a giant impact. *Science* **338,** 1052–1055 (2012).
11. Cuk, M. & Stewart, S. T. Making the Moon from a fast-spinning Earth: A giant impact followed by resonant despinning. *Science* **338,** 1047–1052 (2012).
12. Dahl, T. W. & Stevenson, D. J. Turbulent mixing of metal and silicate during planet accretion? and interpretation of the Hf–W chronometer. *Earth Planet. Sci. Lett.* **295,** 177–186 (2010).
13. Walker, R. J. Highly siderophile elements in the Earth, Moon, and Mars: Update and implications for planetary accretion and differentiation. *Chem. Erde-Geochem.* **69,** 101–125 (2009).
14. Bottke, W. F., Walker, R. J., Day, J. M. D., Nesvorny, D. & Elkins-Tanton, L. Stochastic late accretion to Earth, the Moon, and Mars. *Science* **330,** 1527–1530 (2010).
15. O'Brien, D. P., Morbidelli, A. & Levison, H. F. Terrestrial planet formation with strong dynamical friction. *Icarus* **184,** 39–58 (2006).
16. Raymond, S. N., O'Brien, D. P., Morbidelli, A. & Kaib, N. A. Building the terrestrial planets: Constrained accretion in the inner solar system. *Icarus* **203,** 644–662 (2009).
17. Stewart, S. T. & Leinhardt, Z. M. Collisions between gravity-dominated bodies. II. The diversity of impact outcomes during the end stage of planet formation. *Astrophys. J.* **751,** 32 (2012).
18. Ahrens, T. J. & O'Keefe, J. D. Shock melting and vaporization of lunar rocks and minerals. *Moon* **4,** 214–249 (1972).
19. Kraus, R. G. *et al.* Shock vaporization of silica and the thermodynamics of planetary impact events. *J. Geophys. Res.* **117,** E09009 (2012).
20. Nellis, W. J. & Yoo, C. S. Issues concerning shock temperature measurements of iron and other metals. *J. Geophys. Res.* **95,** 21749–21752 (1990).
21. Hixson, R. S., Winkler, M. A. & Hodgdon, M. L. Sound speed and thermophysical properties of liquid iron and nickel. *Phys. Rev. B* **42,** 6485–6491 (1990).
22. Beutl, M., Pottlacher, G. & Jager, H. Thermophysical properties of liquid iron. *Int. J. Thermophys.* **15,** 1323–1331 (1994).
23. Kerley, G. I. *Multiphase Equation of State for Iron. Tech. Rep.* SAND93-0027 (Sandia National Laboratories, 1993).
24. Anzellini, S., Dewaele, A., Mezouar, M., Loubeyre, P. & Morard, G. Melting of iron at Earth's inner core boundary based on fast x-ray diffraction. *Science* **340,** 464–466 (2013).
25. Thompson, S. L. & Lausen, H. S. *Improvements in the CHARTD Radiation-Hydrodynamic Code III. Revised Analytic Equation of State. Tech. Rep.* SC-RR-710714 (Sandia National Laboratories, 1972).
26. Johnson, B. & Melosh, H. Formation of spherules in impact produced vapor plumes. *Icarus* **217,** 416–430 (2012).
27. Harper, C. L. & Jacobsen, S. B. Evidence for ^{182}Hf in the early solar system and constraints on the timescale of terrestrial accretion and core formation. *Geochim. Cosmochim. Acta* **60,** 1131–1153 (1996).
28. Jacobsen, S. B. & Harper, C. L. in *Earth Processes: Reading the Isotopic Code* (eds Basu, A. & Hart, S.) 47–74 (American Geophysical Union, 1996).
29. Savage, M. E. *et al. 2007 IEEE Pulsed Power Conference* Vol. 2, 979 –984 (IEEE, 2007).
30. Brown, J. M., Fritz, J. N. & Hixson, R. S. Hugoniot data for iron. *J. Appl. Phys.* **88,** 5496–5498 (2000).

Acknowledgements

Sandia National Laboratories is a multiprogram laboratory managed and operated by Sandia Corporation, a wholly owned subsidiary of Lockheed Martin Corporation, for the US Department of Energy's National Nuclear Securities Administration under Contract No. DE-AC04-94AL85000. This work was conducted under the Sandia Z Fundamental Science Program and supported by the Department of Energy National Nuclear Security Administration under Award Number DE-NA0001804. This work was improved by helpful discussions with R. Walker, D. Flicker, D. Swift, M. Knudson and M. Desjarlais. We thank S. Raymond, K. Walsh and D. O'Brien for the impact data from their N-body simulations. Iron samples were provided by B. Jensen of Los Alamos National Laboratory.

Author contributions

R.G.K. conceived the experimental technique. R.G.K., S.T.S., S.B.J. and T.R.M. prepared the proposal for experimental time. S.R., R.W.L. and R.G.K. designed and conducted the experiments. R.G.K. analysed the data. R.G.K. and S.T.S. wrote the paper and all authors provided comments on the manuscript.

Additional information

Supplementary information is available in the online version of the paper. Reprints and permissions information is available online at www.nature.com/reprints. Correspondence and requests for materials should be addressed to R.G.K.

Competing financial interests

The authors declare no competing financial interests.